ACS APPLIED MATERIALS & INTERFACES

Research Article

www.acsami.org

# Effect of Surface Compositional Heterogeneities and Microphase Segregation of Fluorinated Amphiphilic Copolymers on Antifouling Performance

Zeliang Zhao,[†] Huagang Ni,*[,†] Zhiyuan Han,[†] Tengfei Jiang,[†] Yongjuan Xu,[†] Xiaolin Lu,[‡] and Peng Ye*[,†]

[†]Department of Chemistry, Key Laboratory of Advanced Textile Materials and Manufacturing Technology of Education Ministry, Zhejiang Sci-Tech University, Hangzhou 310018, China

[‡]State Key Laboratory of Bioelectronics, School of Biological Science and Medical Engineering, Southeast University, Nanjing, 210096, China

Supporting Information

**ABSTRACT:** In this paper, a series of fluorinated amphiphilic copolymers composed of 2-perfluorooctylethyl methacrylate (FMA) and 2-hydroxyethyl methacrylate (HEMA) monomers were prepared, and their surface properties and antifouling performance were investigated. Bovine serum albumin (BSA) and human plasma fibrinogen (HFg) were used as model proteins to study protein adsorption onto the fluorinated amphiphilic surfaces. All the fluorinated amphiphilic surfaces exhibit excellent resistant performance of protein adsorption measured by X-ray photoelectron spectroscopy (XPS). The surface compositional heterogeneities on the molecular scale play an important role in the antifouling properties. It was found that the copolymers exhibited better antifouling properties than the corresponding homopolymers did, when the percentage of hydrophilic hydroxyl groups is from 4% to 7% and the percentage of hydrophobic fluorinated moieties is from 4% to 14% on the surface. In addition, the protein molecular size scale and the pattern of microphase segregation domains on the surface strongly affect the protein adsorption behaviors. These results demonstrate the desirable protein-resistant performance from the fluorinated amphiphilic copolymers and provide deeper insight of the effect of surface compositional heterogeneity and microphase segregation on the protein adsorption behaviors.

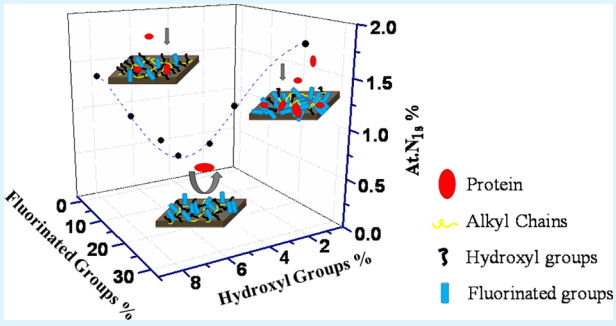


**KEYWORDS:** *fluorinated amphiphilic surface, protein adsorption, surface composition, heterogeneity, microphase segregation*

## INTRODUCTION

Protein adsorption at solid surfaces plays a critical role in many biological phenomena and has aroused a wide range of interest for researchers. In spite of considerable progress in this area, there were still widely differing and even contradictive reports on how to understand such phenomena like protein aggregation, overshooting adsorption kinetics, and structural rearrangements.[1] Nonspecific adsorption for protein and associated bioadhesion is one of the most significant limitations to the end point utility of many infrastructures and devices like food industries, marine ship hulls, biomedical implants, etc.[2−6] The adsorbed quantities and conformations of proteins strongly depend on the chemical and physical properties of the substrate surfaces. Therefore, it is necessary to develop antifouling polymer surfaces with optimum surface structures for the purpose of preventing unwanted accumulation of bioadhesion and protein adsorption at surfaces and interfaces.

There have been considerable studies on designing and fabricating antibiofouling materials when contacted with physiological or biological fluids. In general, the increase in hydrophilicity always benefits to enhance fouling resistance since many foultants (like proteins) are hydrophobic in nature.[7,8] Hydrophilic materials[9−14] like oligo(ethylene glycol) (OEG) or poly(ethylene glycol)(PEG) possess a low water/material interfacial energy and mainly acquire surface hydration via hydrogen bonds, while zwitterionic materials like poly(carboxybetaine methacrylate) and poly(sulfobetaine methacrylate) achieve surface hydration via ionic-induction in which the water molecules are bound even more strongly. Fluoropolymers have also been investigated as antifouling coatings in that their low surface energies can significantly reduce the polar and hydrogen bonding interactions with the fouling organisms or cause the feasible release of the fouling organisms from the coating surfaces.[15−18] For example, Kawakami reported that fluorinated polyimide can suppress protein adsorption for its high surface hydrophobicity and low surface free energy.[19,20] In addition, we found that the well ordered and perpendicularly oriented structure of the

Received: April 27, 2013
Accepted: July 23, 2013
Published: July 23, 2013

  

**Scheme 1. Synthesis Route of PHEMA-*r*-PFMA Copolymers**

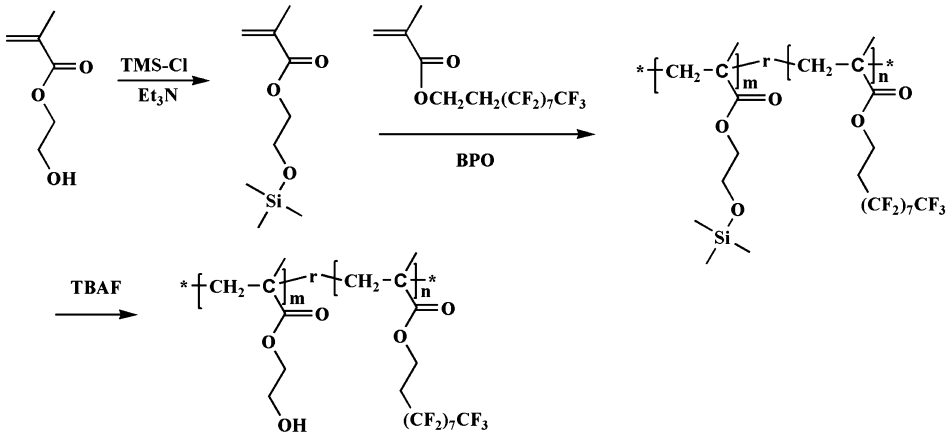


perfluoroalkyl groups on the support surface was correlated with excellent antifouling property of fluorinated poly(methyl methacrylate) copolymers.[18] In brief, the antifouling performances strongly depend on the physicochemical properties of the support surfaces (such as, surface chemistry, surface morphology, and surface charge).

Amphiphilic polymers with their dual nature can resist biofouling by providing the surface with a morphological, topological, and compositional complexity, which either reduces adhesion of the motile microorganism or makes energetically unfavorable the hydrophilic or the hydrophobic interactions between the supports with organism's adhesives.[21,22] It was found that the coatings obtained from fluorocarbon and saturated PEG copolymers exhibited better repellence of protein adsorption than the hydrophobic fluorocarbon coatings.[6,23] It was reported that the surface tethered with hyperbranched polymers containing both PEGylated and fluorinated groups exhibited low protein adsorption and high fouling-release properties when the composition of hydrophobic and hydrophilic monomers was at an optimal ratio.[24,25] The comblike amphiphilic block copolymer poly(ethoxylated fluoroalkyl acrylate)−polystyrene with ethoxylated fluoroalkyl side chains showed very high removal of both *Ulva* sporelings and diatom Navicula.[26,27] Feng et al. and Joshi et al. took a similar strategy to prepare antifouling surfaces by using polyurethane−polyol and perfluoroether−PEG amphiphilic copolymers.[28−30] Following researchers had then built on this strategy of constructing amphiphilic surfaces for controlling biofouling and demonstrated the broad applicability of this strategy.[31−37] These systems clearly indicated that nanostructured, amphiphilic surfaces with mixed hydrophilic and fluorinated properties performed better than the corresponding hydrophilic and fluorinated polymer surfaces.[37]

It has been speculated that the nonfouling or fouling-release characteristics of these amphiphilic materials arises from nanoscale variations in the surface chemistry, topography, and mechanical properties.[7,32,38] The concept of "ambiguous" surfaces where the phase-segregation occurs to produce to mosaics of hydrophilic and hydrophobic domains has been developed based on the above statement. It is believed that these ambiguous surfaces with compositional heterogeneities on the foulant-length scale may make thermodynamically unfavorable interactions between the surface and the foulant, which then might limit adsorption events.[35,39] Since adsorbed proteins as a class of important foulant can subsequently arouse adhesion of cells or microorganisms onto the surface, so the surface that reduces the adhesion of protein could potentially resist other foulants.[39,40] The surfaces with compositional heterogeneities over molecular-length scales were designed to enhance the repellence to protein adsorption.[39] The thin films of random copolymers composed of highly hydrophobic and highly hydrophilic monomers were prepared by photoinitiated chemical vapor deposition (piCVD), which could obviously disrupt surface−protein interactions and therefore strengthen repellence to the protein adsorption.[40] Chen[41] reported that amphiphilic homopolymers with incompatible hydrophobic and hydrophilic functionalities on the special molecular-scale alternation could obviously reduce protein adsorption. However, some investigations revealed that amphiphilic copolymer surfaces did not always own molecular-scale compositional heterogeneities or exhibit improvement of protein-resistant performance.[38]

Inspired by these successful strategies against protein adsorption, we made effort to fabricate compositional heterogeneities on the molecular scale for resisting proteins adsorption. The polymer films at the molecular-level heterogeneities in surface composition can be achieved via amphiphilic random copolymers composed of hydrophobic and hydrophilic monomers. However, it is difficult to obtain the copolymers by polymerization of hydrophilic and hydrophobic monomers due to their immiscibility and different reactivity ratio.[42−44] It was reported that fluorinated acrylates with hydrophilic acrylates could be copolymerized, but the thin film surfaces prepared by a solution cast method were extremely rough and nonuniform.[45,46] Although smooth, thin polymer films could be obtained by utilizing piCVD, the hydroxyl groups of hydroxyethylmethacrylate (HEMA) inevitably got cross-linked under an UV light so as to weaken hydrophilic properties to some degree.[39]

In this study, the smooth, thin copolymer films with compositional heterogeneity on the individual monomer molecular size scale were prepared by using fluorinated amphiphilic copolymers composed of hydrophilic 2-hydroxyethyl methacrylate (HEMA) and hydrophobic 2-perfluorooctylethyl methacrylate (FMA). Copolymers P(HEMA-*r*-FMA) were synthesized by deprotection after the random free radical copolymerization of FMA and HEMA in the protected form of trimethylsilanes (TMS) for avoiding the cross-linked reaction of −OH groups from HEMA during

polymerization (as shown in Scheme 1).[47] By varying the monomer ratio of HEMA to FMA, copolymers with a wide range of composition could be acquired. The amphiphilic random copolymer films were made by spin-coating and characterized by atomic force microscopy (AFM) and X-ray photoelectron spectroscopy (XPS). The protein-resistant properties of fluorinated amphiphilic copolymer films were then evaluated with bovine serum albumin (BSA) and human plasma fibrinogen (HFg) as model proteins.

## EXPERIMENTAL SECTION

**Materials.** 2-Perfluorooctylethyl methacrylate (FMA) (Sigma-Aldrich) was purified by washing with sodium hydroxide solution, dried through calcium hydride ($CaH_2$), and vacuum-distilled before use. Trimethyl chlorosilane (TMS-Cl) was purchased from Sigma-Aldrich and used as received. Triethylamine (TEA, Gaojing fine chemical Co., Hangzhou China) was distilled from $CaH_2$. Benzoyl peroxide (BPO) was recrystallized from methanol. Prior to use, toluene was dried by refluxing in the presence of sodium. According to the report,[48] 2-hydroxyethyl methacrylate (HEMA) was purified by washing an aqueous solution (25 vol %) of HEMA with *n*-hexane, salted from the aqueous phase by addition of sodium chloride, dried through magnesium sulfate, and then vacuum distilled. Human plasma fibrinogen (HFg) and bovine serum albumin (BSA) were purchased from Shanghai Jianglai Co., Shanghai, China. Poly(methyl methacrylate) (PMMA) ($M_w$ = 100 000) was acquired from Polymer Source Corp. The other solvents and chemicals were used as received.

Fluorinated amphiphilic random copolymers were synthesized with a three-step method as shown in Scheme 1. At first, the hydroxyl in HEMA monomer was protected to form a hydrophobic monomer (HEMA-TMS); then, P(HEMA-TMS)-*r*-PFMA copolymers were prepared via radical copolymerization initiated by BPO; finally, fluorinated amphiphilic random copolymers (PHEMA-*r*-PFMA) were synthesized by the hydrolysis reaction of the P(HEMA-TMS)-*r*-PFMA copolymers.

**Synthesis of 2-(Triethylsiloxy)ethyl Methacrylate (HEMA-TMS).** HEMA-TMS was prepared according to the literature.[49] A dry 1 L round-bottom flask with a mechanical stirring rod was vacuumized and charged with dry nitrogen three times, then cooled to 0 °C. An 80 mL (0.6 mol) portion of purified HEMA, 85 mL (0.6 mol) TEA, and 500 mL ethyl ether were added, respectively. Then, 78 mL (0.6 mol) TMS-Cl was added within 30 min. The reaction mixture was sequentially stirred at 0 °C for 2 h. After reaction, the mixture was filtered for removing the solid precipitate. The solid was washed with ethyl ether two times, filtrated, and washed with 100 mL deonized water three times. The oil layer separated was dried over $MgSO_4$ and distilled to remove ethyl ether. The protected monomer was distilled under vacuum (50 °C, 0.06 Torr). Yield: 70%. $^1$H NMR ($CDCl_3$, $\delta$ in ppm): 0 (s, 9H, $-Si(C\underline{H}_3)_3$), 2.0 (s, 3H, $CH_2{=}C(C\underline{H}_3)COO-$), 3.9 (t, 2H, $-CH_2C\underline{H}_2O-Si(CH_3)_3$), 4.3 (m, 2H, $-C\underline{H}_2CH_2O-Si(CH_3)_3$), 5.6, 6.1 (m, 2H, $C\underline{H}_2{=}C(CH_3)COO-$).[49]

**Synthesis of P(HEMA-TMS)-*r*-PFMA Random Copolymers.** The molar ratios of 2-(triethylsiloxy)ethyl methacrylate to fluorinated monomer (FMA) are 97:3, 94:6, 91:9, 88:12, 85:15, and 70:30 in the reaction mixtures during radical copolymerization, respectively. The following are typical reaction conditions. In a dry 100 mL Florence flask, 10 mL (50 mmol) HEMA-TMS, 1.1 mL (3 mmol) FMA, and 30 mL toluene were added one by one, after nitrogen was purged into the flask to remove the air atmosphere, the initiator BPO was added subsequently. The mixture was kept at 70 °C for one day with stirring. Afterward, the polymer solution was concentrated and diluted with tetrahydrofuran (THF). Water was injected into the solution for precipitation, and the resulting product P(HEMA-TMS)-*r*-PFMA was obtained and dried in vacuo at 25 °C.

**Preparation of PHEMA-*r*-PFMA Fluorinated Amphiphilic Random Copolymers.** Fluorinated amphiphilic random copolymers were prepared by hydrolysizing P(HEMA-TMS)-*r*-PFMA with tetrabutylammonium fluoride (TBAF). The procedure was as follows: 5g P(HEMA-TMS)-*r*-PFMA was dissolved in 30 mL tetrahydrofuran, then transferred into a 100 mL Florence flask containing a magnetic stir bar. TBAF/THF (w/v = 1/1) was slowly introduced into the solution in the flask. The reaction then ran at 25 °C with continuous stirring for 5 h. The mixture was precipitated into deionized water.[50] The precipitate was washed with deionized water and dried in vacuo at 25 °C. The molar content of PFMA in the resulting PHEMA-*r*-PFMA copolymers are 2.45%, 4.90%, 7.56%, 10.07%, 13.70%, and 26.73% according to the calculation of the fluorine element analysis results, respectively (as shown in Table 1). The monomer ratios in reaction mixtures are good correlations with the monomer composition in copolymers.

**Table 1. Characteristics of PHEMA-*r*-PFMA and P(HEMA-TMS)-*r*-PFMA Copolymers**

| | P(HEMA-TMS)-*r*-PFMA | | PHEMA-*r*-PFMA | | |
|---|---|---|---|---|---|
| sample | $M_n^1 \times 10^{-4}$ [a] | $M_w/M_n$ [a] | $M_n^2 \times 10^{-4}$ [b] | $W_F$ (%) [c] | FMA (mol %) [d] |
| F1 | 4.81 | 1.96 | 3.20 | 5.65 | 2.45 |
| F2 | 4.99 | 1.70 | 3.43 | 10.59 | 4.90 |
| F3 | 5.15 | 1.97 | 3.64 | 15.23 | 7.56 |
| F4 | 4.93 | 1.99 | 3.57 | 19.05 | 10.07 |
| F5 | 4.84 | 1.91 | 3.62 | 23.91 | 13.70 |
| F6 | 4.56 | 2.10 | 3.73 | 36.36 | 26.73 |

[a]Determined by GPC. [b]Calculated from GPC and PHEMA-*r*-PFMA. [c]Obtained from EA. [d]Calculated from PHEMA-*r*-PFMA.

**Film Formation.** The glass slides (10 mm × 10 mm) used as substrates were cleaned by immersion a piranha solution (1:3 v/v 30% aq $H_2O_2$/conc $H_2SO_4$) for 30 min, rinsed well with deionized water, and dried. All polymers were dissolved in *N*,*N*-dimethylformamide (DMF) to make the concentration of 2 wt %, then the solution was filtered using a porous filter (0.45 $\mu$m aperture diameter). Polymer films were obtained by spin-coating the polymer solution onto the clean glass slides at 2500 r/min for 30 s and then drying in vacuo at 40 °C for 72 h to remove the residual solvent. The PHEMA film was prepared according to the literature.[51,52] Soluble poly(HEMA) (Sigma-Aldrich, $M_v$ 20 000) was spin-coated from solution onto the glass slides which previously coated with an ethyl methacrylate /($\gamma$-methacryloxypropyl)trimethoxysilane copolymer (2.5% EMA-silane in ethyl acetate) as a coupling agent. PHEMA solution (2 wt %) with DMF as solvent was spin-coated at 2500 r/min for 30 s on the EMA-silane treated glass and then dried in vacuo at 40 °C for 72 h.

**Characterization.** $^1$H NMR spectra were recorded with a Bruker Avance AMX-400 NMR spectrometer in deuterated dimethyl sulfoxide (DMSO-$d_6$) or deuterated chloroform ($CDCl_3$) with tetramethylsilane (TMS) as the internal standard. The FTIR spectra of the polymer films on KBr plates cast from solutions were collected using a Nicolet Avatar 370 Fourier transform infrared (FTIR) spectrometer. The molecular weights and molecular weight distributions (MWDs) of copolymers were measured on a Waters 1515 gel permeation chromatography (GPC) apparatus (with THF as eluent at a flow rate of 0.8 mL/min at 35 °C). The instrument was calibrated with polystyrene (PS) standards. The composition of copolymers was determined by $^1$H NMR and fluorine elemental analysis (F-EA). Fluorine analyses were carried out by flask combustion and then followed by ion chromatography on an Elementar vario EL III instrument.[53]

Water contact angles ($\theta$) were measured using a contact angle goniometer (DSA-10, Krüss, Hamburg, Germany) at room temperature and ambient humidity. The contact angles ($\theta$) given are the averages of at least eight separate measurements on different areas of polymer surfaces. The contact angles of diiodomethane on polymer films were detected, and then the surface free energy of various samples was estimated according to the theory of Owens and Wendt.[54]

X-ray photoelectron spectroscopy (XPS) measurements were carried out on a PHI5000C ESCA system with an Mg Ka X-ray

source at a power of 250 W (140 kV) under a vacuum of $1.0 \times 10^{-8}$ Torr with a takeoff angle of 54°. Three different sites on per sample were measured, each measurement included a survey with three sweeps, and a high-resolution measurement for $N_{1s}$ consists of eight sweeps. The $C_{1s}$ peak of the C−C bond at 284.6 eV was used as the reference for binding energy calibration of all spectra.[18]

Tapping-mode AFM measurements were performed using a scanning probe microscopy (Veeco Dimension 5000 with Nanoscope V controller, Digital Instruments, Inc.). Silicon AFM tips with a tip radius of 10 nm (NSC 15/AIBS, MikroMasch, Estonia) were used. The polymer surface coated on a 10 mm ×10 mm glass wafer was scanned at 1.5 Hz. All images were post-treated with Nanoscope 5.31r1 software.

**Protein Adsorption Measurement.** BSA and HFg were used as model proteins to evaluate the protein-resistant performance of the polymeric films. The protein adsorption experiments were performed according to the literature.[18,41] The polymer films (on glass slides) were immersed in deionized water for 30 min, and then, the samples were transferred into vials containing 0.1 mg/mL protein (BSA or HFg) in PBS buffer solution (~pH 7.4) and incubated at room temperature for 2 h. The samples were removed from the vials and rinsed with PBS buffer solution and deionized water three times, respectively, to remove any unbound or loosely bound proteins. After that, the samples were dried by nitrogen. Protein adsorbed on the samples were measured by XPS and calculated by integration of the peak area of the $N_{1s}$ peak from the corresponding XPS spectra.[18]

## RESULTS AND DISCUSSION

**Fluorinated Amphiphilic Copolymers Synthesis and Characterization.** In order to avoid the cross-linking reaction of −OH in PHEMA during copolymerization and obtain various compositional heterogeneous copolymers, the amphiphilic copolymers poly(hydroxyethylmethacrylate)-*r*-poly(2-perfluorooctyl methacrylate)s (PHEMA-*r*-PFMA) were synthesized as illustrated in Scheme 1. At first, the hydrophobic monomer 2-(trimethylsiloxy)ethyl methacrylate (HEMA-TMS) was synthesized by protecting the hydroxyl group of HEMA with a trimethylsilyl group (TMS-Cl). The less polar HEMA-TMS with the similar solubility in common solvent compare to FMA can be copolymerized with FMA readily using a common condition by free radical polymerization.[49] Then fluorinated amphiphilic copolymer PHEMA-*r*-PFMA was synthesized by the hydrolysis reaction of the P(HEMA-TMS)-*r*-PFMA copolymer. Due to the intrinsic association[55,56] of the FMA units, it is difficult to characterize the fluorinated monomer content in copolymers by $^1$H NMR. Thus the fluorinated monomer content was determined by elemental analysis.[57] The molar content of fluorinated monomer (FMA mol %) in PHEMA-*r*-PFMA was calculated according the following eq 1-1:

$$\text{FMA (mol \%)} = \frac{M_{\text{HEMA}} W_{\text{F}}\%}{19 \times 17 + M_{\text{HEMA}} W_{\text{F}}\% - M_{\text{FMA}} W_{\text{F}}\%} \quad (1\text{-}1)$$

Where $W_{\text{F}}$ is the content of fluorine element, $M_{\text{HEMA}}$ and $M_{\text{FMA}}$ are the molecular weight of 2-hydroxyethyl methacrylate and 2-perfluorooctyl methacrylate, respectively. The molecular weight and polydispersity of P(HEMA-TMS)-*r*-PFMA can be determined by GPC. Because the fluorinated amphiphilic copolymers PHEMA-*r*-PFMA are indissoluble in THF, it is hard to determine the molecular weight directly by GPC measurement. With a view to complete hydrolyzation of the protected form of trimethylsilanes (TMS) in PHEMA, the molecular weight of PHEMA-*r*-PFMA can be obtained according to the molecular composition and content of FMA in P(HEMA-TMS)-*r*-PFMA with the following equation 1-2:

$$M_{\text{PHEMA-}r\text{-PFMA}} = M_{\text{P(HEMA-TMS)-}r\text{-PFMA}} \times \left[1 - \frac{72(1 - \text{FMA mol \%})}{M_{\text{HEMA-TMS}}(1 - \text{FMA mol \%}) + M_{\text{FMA}}\text{FMA mol \%}}\right] \quad (1\text{-}2)$$

$M_{\text{HEMA-TMS}}$, $M_{\text{P(HEMA-TMS)-}r\text{-PFMA}}$, and $M_{\text{PHEMA-}r\text{-PFMA}}$ represent the molecular weight of HEMA-TMS, P(HEMA-TMS)-*r*-PFMA, and PHEMA-*r*-PFMA, respectively. Table 1 show all the copolymers used in this study. Every sample with different fluorine content is named F1−F6 for short, and F0 in this study represents PHEMA homopolymer. All the samples have the similar molecular weight.

The fluorinated amphiphilic copolymers synthesized using the above methods were characterized by FTIR. The FTIR spectra of P(HEMA-TMS)-*r*-PFMA and PHEMA-*r*-PFMA are shown Figure 1. The absorbance for C−F stretching vibration

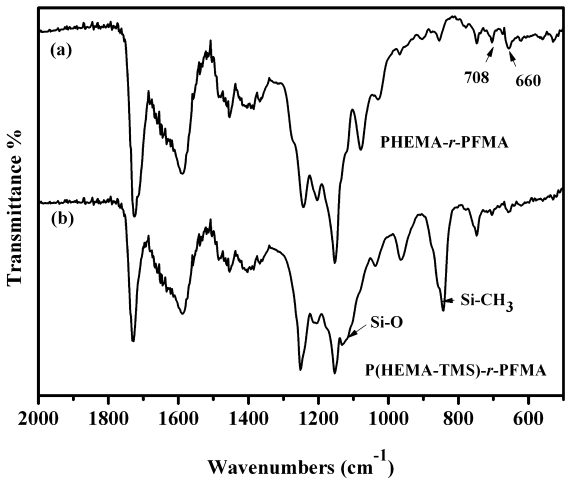


**Figure 1.** FTIR spectra of PHEMA-*r*-PFMA (a) and P(HEMA-TMS)-*r*-PFMA (b) copolymers: 7.5 mol % FMA in copolymer.

bands around 1200−1270 $cm^{-1}$ overlaps with the C−O stretching vibration band around 1270−990 $cm^{-1}$. Two medium bands which resulted from a combination of rocking and wagging vibrations of $CF_2$ groups are at 660 and 708 $cm^{-1}$, respectively.[57−59] The absorbance at 840 $cm^{-1}$ for Si−$CH_3$ stretching vibration band and at 1104 $cm^{-1}$ for Si−O stretching vibration band disappear after hydrolysis, and a broad hydroxyl peak around 3500 $cm^{-1}$ (not show) can be observed in PHEMA-*r*-PFMA.[39]

When the fluorinated monomer contents are higher, the structures of fluorinated random copolymers can be characterized by $^1$H NMR. The $^1$H NMR spectra of PHEMA-*r*-PFMA and P(HEMA-TMS)-*r*-PFMA are shown in Figure S1 (Supporting Information). Both PHEMA-*r*-PFMA and P(HEMA-TMS)-*r*-PFMA show two methylene proton peaks at 3.9 (−C$\underline{H}_2$CH$_2$OH) and 3.6 ppm (−CH$_2$C$\underline{H}_2$OH), and a small peak observed at around 4.23 ppm is attributed to the protons of −OC$\underline{H}_2$CH$_2$(CF$_2$)$_7$CF$_3$ in the FMA unit.[59,60] When the integral area of hydroxyl peak at 4.8 ppm (−CH$_2$O$\underline{H}$) is 1/2 that of peak at 3.9 ppm (−C$\underline{H}_2$CH$_2$OH) and the peak of Si(CH$_3$)$_3$ units at 0 ppm is absent, which indicates the complete removal of TMS group resulting in pure PHEMA-*r*-PFMA.[61] These results indicate that amphiphilic random

copolymers PHEMA-*r*-PFMA with various content of PFMA (listed in Table 1) were synthesized successfully.

**Surface Structure of the Fluorinated Amphiphilic Copolymer Films.** The static water contact angles on the PHEMA-*r*-PFMA films with different FMA content in copolymers and the corresponding surface free energies are illustrated in Figure 2. The water contact angle of PHEMA

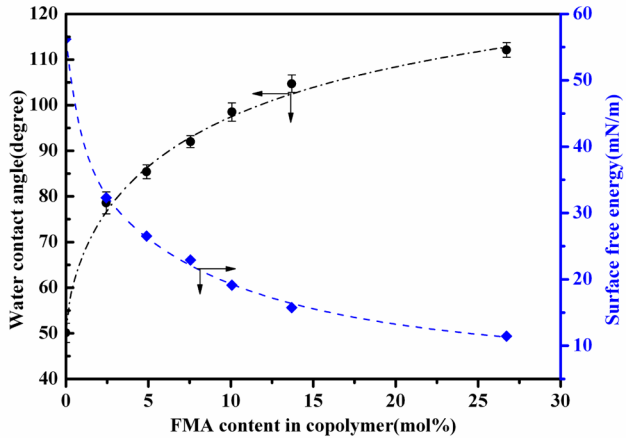


**Figure 2.** Static water contact angles and surface free energies as a function of amphiphilic copolymers.

homopolymer is about 50° as same the report.[39] With increasing of hydrophobic content, the contact angle of copolymer increases rapidly and reached 112° at 26.7 mol % FMA close to the value for PFMA homopolymer.[62] Simultaneously, the surface free energies of PHEMA-*r*-PFMA films as a function of composition are depicted in Figure 2. The surface free energies of random copolymer PHEMA-*r*-PFMA film surface decrease from 56.2 to 11.4 mN/m with increasing of incorporation of FMA in copolymer. HEMA with a pendant hydroxyl group is hydrophilic, while FMA containing the fluorinated alkyl side chain is highly hydrophobic and its surface energy is lower than poly(tetrafluoroethylene) (PTFE).[39,62] It is generally accepted that the chemical structures and physical roughness of polymer film surfaces determine the wetting behaviors of polymer surfaces.[63] Tapping model atom force microscopy (AFM) was used to examine the surface roughness of those polymer films. All the films have a very smooth and flat surface, with RMS roughness values of all films less than 3 nm. This indicates that the effect of physical roughness can be negligible.[57,63] It means that various surface structures of fluorinated amphiphilic polymer films were obtained through varying the composition of random copolymers.

It was shown that fluorine moieties which occurred in the topmost layer of the surface within 1−2 nm determine the surface free energy of polymer films.[18,59] Although the films prepared by spin-coating are only about 80 nm thick, the film's bulk composition can not reflect film's surface chemical composition. The hydrophobic fluorinated species of FMA will preferentially occupy the films outermost surface, while the hydrophilic hydroxyl group of HEMA will be likely to orient inward, in air or vacuum conditions.[39] It is necessary to provide direct evidence of the surface segregation of perfluorinated and oxygen-containing polar groups for interpreting the wettability change of these copolymer surfaces.

The surface composition of amphiphilic copolymers was probed via XPS measurements. Figure 3 shows the XPS spectra

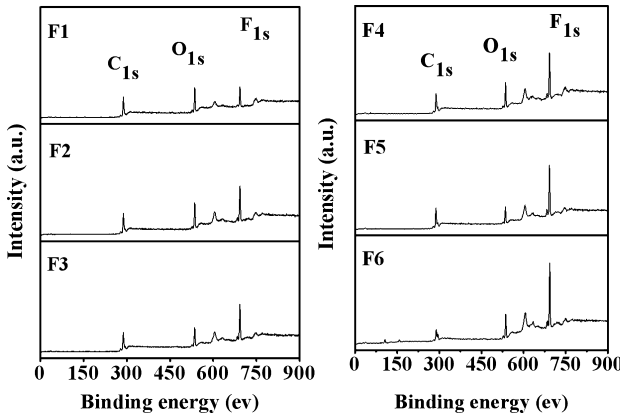


**Figure 3.** XPS spectra of the PHEMA-*r*-PFMA films recorded at a takeoff angle of 54°.

of the PHEMA-*r*-PFMA films prepared by spin-coating. The $F_{1s}$ peak occurs at about 689 eV. The peak at 531 eV is attributed to $O_{1s}$. Meanwhile the $C_{1s}$ peak occurs at 285 eV.[57,64] It can be seen that the content of fluorine moieties on the copolymer surface increase with increasing content of FMA in bulk. The oxygen and fluorine enrichment, i.e., the oxygen to carbon atomic ratios (O/C) and the fluorine to carbon atomic ratios (F/C) at the outermost film surface measured by XPS are given in Table 2. The XPS $C_{1s}$ high resolution spectra were recorded for further investigating the composition of functional groups on the film surfaces.

Figure 4 shows high resolution $C_{1s}$ XPS scans of amphiphilic copolymers PHEMA-*r*-PFMA with different fluorinated content at a takeoff angle of 54°. The various carbon-based functional groups are attributed to the corresponding discrete peaks, and the composition ratios (listed in Table 2) are calculated from corresponding peak areas of the carbon components. The $C_{1s}$ XPS spectra were resolved into six Gauss fitted peaks: the strong intensity peak C—C around 284.6 eV, indicative of the copolymer backbone, peaks near 294 and 292 eV representing —$CF_3$ and —$CF_2$ respectively, —C═O (288.4 eV) and —COC═O (287.6 eV) with the same integral area, and 286.2 eV associated with —C—O present attributing to the hydroxyl ethyl group which also is taken for hydrophilic hydroxyl group moieties. These peak assignments agree well with previously reported values.[65] As shown in Figure S2 (Supporting Information), it is obvious that the content of fluorinated species ($CF_2$ group) on the surface and in bulk increase with the increasing content of PFMA in the copolymer. In addition, the fluorinated species ($CF_2$ group) content on the film surface is higher compare to that in bulk. These also indicate that the change of wettability of fluorinated amphiphilic copolymer PHEMA-*r*-PFMA is stemmed from the surface composition alteration.

The surface phase images of the amphiphilic copolymers were investigated with AFM. Because of incompatibility and the obvious difference in the surface energy between the non-fluorinated species and fluorinated components, the fluorinated components can readily enrich at the surface and result in the obvious phase-segregated domains on the surface even when the fluorine moieties are very low in the copolymer.[66,67] The film surfaces in phase mode are shown in Figure 5, which distinguishes between hard and soft materials in the nanoscale. Compared to PHEMA (F0, image A), PFMA performs a hard feature and shows a bright domain. The area of the bright

**Table 2. Surface Element and Composition of PHEMA-*r*-PFMA Copolymer Films**

| | element ratio | | surface composition (%) | | | | | |
|---|---|---|---|---|---|---|---|---|
| sample | $F_{1s}/C_{1s}$ | $O_{1s}/C_{1s}$ | $-CF_3$ | $-CF_2$ | —C═O | —COC═O | —C—O | C—C/C—H |
| F0 | | 0.43 | | | 10.8 | 10.8 | 8.0 | 70.4 |
| F1 | 0.15 | 0.41 | 0.1 | 3.8 | 8.6 | 8.6 | 6.8 | 72.1 |
| F2 | 0.26 | 0.40 | 0.2 | 6.4 | 7.5 | 7.5 | 5.6 | 72.8 |
| F3 | 0.30 | 0.35 | 0.4 | 8.5 | 7.4 | 7.4 | 5.0 | 71.3 |
| F4 | 0.35 | 0.31 | 0.8 | 13.3 | 6.4 | 6.4 | 4.1 | 69.0 |
| F5 | 0.41 | 0.27 | 1.3 | 16.5 | 5.5 | 5.5 | 3.4 | 67.8 |
| F6 | 0.51 | 0.19 | 3.1 | 25.3 | 4.9 | 4.9 | 1.8 | 60.0 |

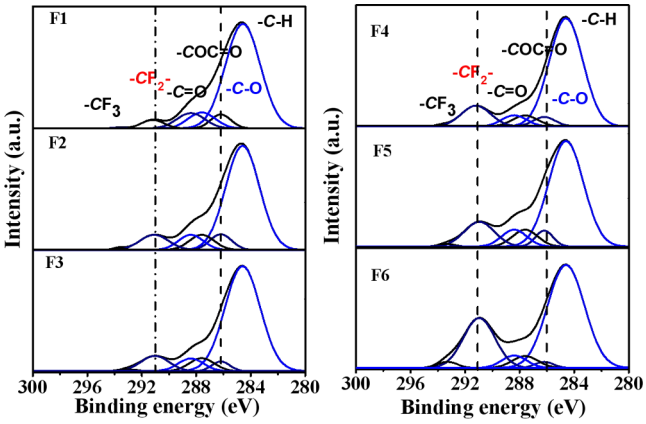


**Figure 4.** XPS $C_{1s}$ core level spectra of PHEMA-*r*-PFMA with different FMA mol % (F1–F6).

domains becomes large with the increase of FMA content on the compositional heterogeneous surfaces. It is obvious that F3 shows an alternating pattern of hydrophilic and fluorinated moieties on the surface, and the interval size is 30–50 nm, which is near the size scale of common proteins. Increasing or decreasing, the content of FMA units will lead to a single dominant factor; therefore, F1 and F5 surfaces exhibit either a large area of hydrophilic domains or more bright phase domains representing the fluorinated moieties. All these AFM results are in accord with XPS and contact angle measurements. These samples with different surface composition and microphase segregation were subsequently used to study the correlation between repellence of protein adsorption and the copolymer surface structures.

**Protein Adsorption on Fluorinated Amphiphilic Polymer Surfaces.** It is always not easy to quantitatively measure protein adsorption on a surface. Conventional methods such as surface plasmon resonance (SPR)[68,69] and quartz crystal microbalance (QCM)[70,71] have their own assumptions upon which its response to the quantity of proteins adsorbed on the prepared coating samples needs to satisfy special requirements. XPS is one simple and effective method to characterize protein adsorption.[41,65,72,73] Wagner et al.[74] analyzed the protein adsorption on hydrogel polymers with XPS and found that there was a detection limit of 10 ng/cm$^2$. Because the polymers do not contain nitrogen atoms, XPS could be easily used to measure adsorbed protein on the surfaces, based on the measurement of 400 eV peak for $N_{1s}$

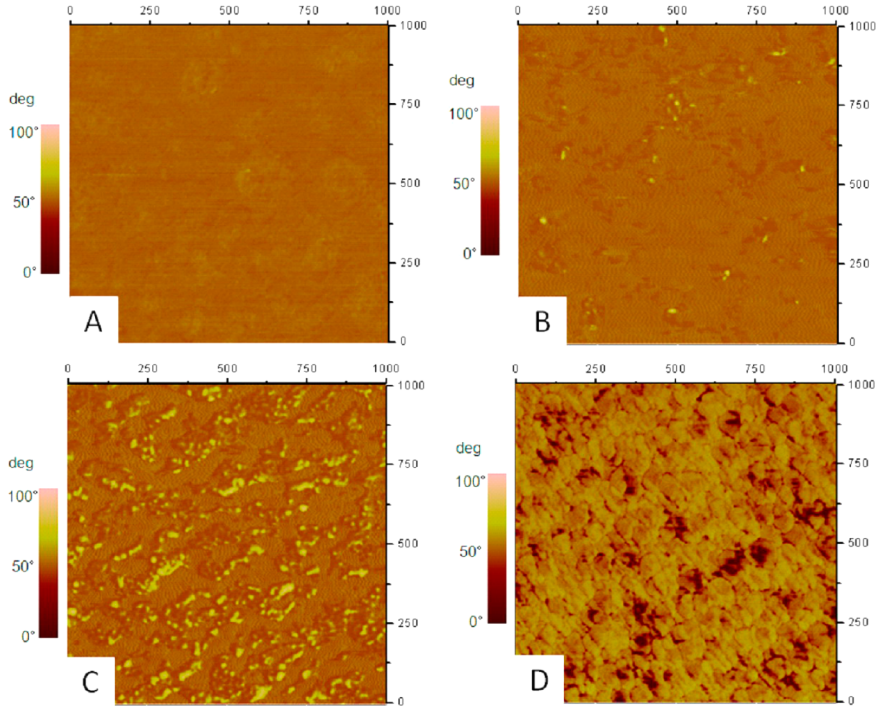


**Figure 5.** AFM tapping phase images (1.0 $\mu$m × 1.0 $\mu$m) of PHEMA-*r*-PFMA films. (A–D) F0, F1, F3, and F5 sample surfaces, respectively.


dx.doi.org/10.1021/am401568b | ACS Appl. Mater. Interfaces 2013, 5, 7808–7818

which could be only from protein.[18] The adsorption behavior of BSA and HFg was studied. The relative intensities of $N_{1s}$ XPS peaks of polymer surfaces are given in Figure S3 (Supporting Information). It is clear that both the hydrophilic homopolymer PHEMA (F0) and the amphiphilic copolymers adsorb less amounts compared with the PMMA homopolymer.

With poly(methyl methacrylate) (PMMA) as a control surface, the adsorption intensity of the surface is regarded as 100%, and other polymer surfaces can be compared with this material.[41] The results are given in Figure 6. It is obvious that

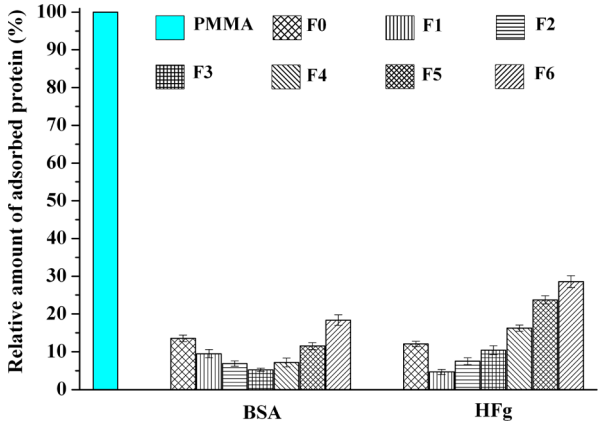


**Figure 6.** Relative amount of adsorbed protein on various surfaces. PMMA was set to 100% as a reference.

all the amphiphilic copolymers exhibit better protein-resistant performance than PMMA. Even for F6 which adsorbs the maximum value of protein compared with other samples, and the value of adsorbed BSA and HFg are 18.4% and 28.6% of that on the PMMA surface, respectively, which indicates PHEMA-*r*-PFMA copolymer surfaces have good antifouling property. It is gratifying for us to see that the amphiphilic sample F3 appears with protein adsorption of only 5%, which is a minimal amount, almost negligible, compared to the common polymer surface. What's more, the F1 surface absorbs only 4.7% HFg. These results show that the existence of the amphiphilic functionalities could reduce protein adsorption. In addition, it is observed that the fluorinated amphiphilic copolymer surfaces exhibit excellent protein resistance greater than the hydrophilic PHEMA surface when fluorinated monomer content is less than 26.3 mol % in the bulk for BSA as a model protein. For HFg adsorption experiments, copolymer surfaces exhibit excellent protein repellence compared to the PHEMA hompolymer surface when FMA content is less than 10.0 mol % in bulk.

PHEMA is a typical antifouling material due to its excellent hydrophilic properties, a water barrier, repelling protein close to the polymer surface.[11,14] In addition, proteins are known to easily adsorb on the hydrophobic surfaces due to the hydrophobic interaction, and this is always detected on the pure hydrophobic surface.[39] Can the increase of hydrophobic content on the support surface actually increase the amount of adsorbed protein on the surface? It is obvious that the hydrophily or hydrophobicity is not the crucial factor for fluorinated amphiphilic copolymer surfaces against the protein adsorption. In fact, bioadhesion is very complex, since many factors such as surface chemistry, surface morphology, and surface charge play important roles.[6] In the early seventies, Baier reported that a critical surface energy in the range of 20−30 mN/m imparted the prevention of marine fouling and resistance of cell adhesion for medical implants in contact with blood.[75,76,27] The experiments of bacteria adhesion were also in accord with the "Baier curve".[77] Bhatt[6] proved that surface energy played an important role; as the amphiphilic PFDA-*co*-DEGVE coatings surface, with surface free energy lying in the range defined by the Baier curve, presented excellent protein repellence. The effect of surface free energy on relative amount of adsorbed protein on the copolymer surfaces is shown in Figure 7.

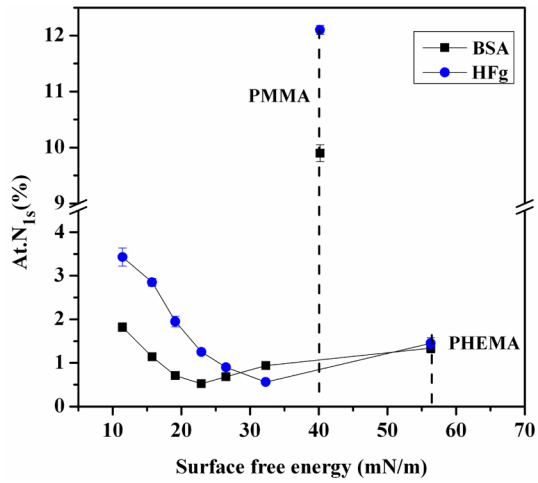


**Figure 7.** Plot of the atom percent of $N_{1s}$ versus surface free energy for PHEMA-*r*-PFMA copolymer surfaces.

With the increase of $F_{1s}/C_{1s}$ ratio and decrease of $O_{1s}/C_{1s}$ ratio on the copolymer surfaces, the corresponding surface free energy decrease. For the fluorinated amphiphilic copolymer, the amount of adsorbed protein does not follow the tendency of the increase or decrease of F/C ratios or O/C ratios or fluorinated species content on the surface (in Table 2 and Figure S2), which signifies a low-attachment surface or a "water barrier" surface, respectively. When the surface free energy is 22.9 mN/m, which is in the surface free energy window where adhesion is minimal, the relative amount of adsorbed BSA is the lowest and even less than that on the PHEMA. However, the $N_{1s}$% value on the surface whose surface free energy is 32.3 mN/m is the minimum for HFg adsorption. Simultaneously, the surface free energy of PMMA is 40.2 mN/m, but the $N_{1s}$% values of on PMMA surface after BSA and HFg adsorption are 9.9% and 12.0%, respectively. Amphiphilc copolymer with surface free energy lying in the range of Baier curve could exhibit excellent repellence of protein adsorption than common polymer with similar surface free energy.

Except for the surface free energy of the copolymers, the surface composition of hydrophobic fluorinated groups and hydrophilic hydroxyl groups may determine the competitive adsorption restrained proteins to approach or adhere. Gleason believed that the smooth surface with compositional heterogeneities on molecular-size scale could obviously disrupt protein adsorption on fluorinated amphiphilic random copolymer films deposited by use of photoinitiated chemical vapor deposition (piCVD).[39] Thünemann reported that a combination SAMs of $CF_3$ and OH groups seriously affected the conformation stabilization of adsorbed HSA compared to SAMs made only of the OH or $CF_3$ thiol.[78] The hydrophobic fluorinated groups are composed of one $CF_3$ headgroup and

seven $CF_2$ groups while the hydrophilic groups represent the hydroxyl ethyl groups. These group compositions are listed in Table 2. The effect the surface group composition on relative amount of adsorbed proteins is shown in Figure 8. It could be

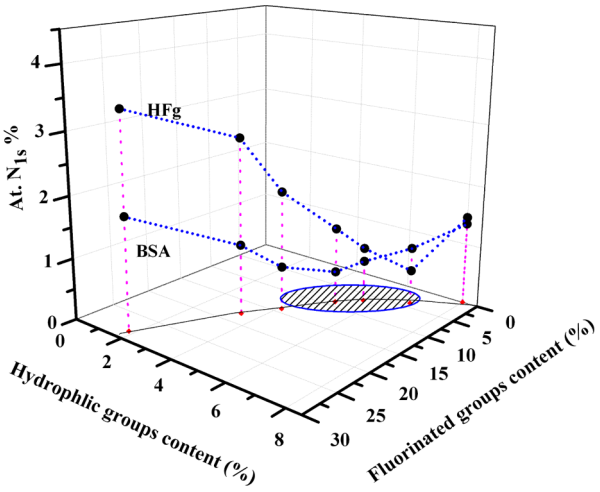


**Figure 8.** Plot of BSA/HFg protein adsorption ratio on PHEMA-*r*-PFMA films with different surface composition.

found that neither the fluorinated group content nor the hydrophilic hydroxyl group content dominates the surface protein-resistant performance individually. That is to say, the surface wettability of these copolymers films is not the crucial effecting factor for protein adsorption behavior. Interestingly, when the fluorinated group content is around 9%, and the hydroxyl group content is around 5% on the surface, BSA adsorbed achieved the lowest; HFg adsorbed the lowest when the fluorinated group content is around 4% and the hydroxyl group content is about 7%. In other words, the minimum amount of adsorbed protein appears in a certain proportion of the surface group's composition. As a result, there should be an appropriate range in the two-dimensional region which is least favorable for protein adsorption, from 4% to 7% hydrophilic hydroxyl groups' content as well as from 4% to 14% hydrophobic fluorinated moieties content than any corresponding homopolymers.

Interestingly, the surface groups' composition of the copolymer adsorbed minimum BSA is different from that adsorbed minimum HFg. The resistant adsorption ability for various proteins may relate with other factors beside surface chemical composition. Protein has both hydrophilic and hydrophobic segments, so proteins can adjust their conformation and orientation according to the adsorbing surface.[6] Although several reports[24,39] described the importance of the amphipathy and "ambiguous surface" for the fluorinated copolymer, it is still an ambiguous understanding of the protein adsorption behavior on amphiphilic fluorinated surface. In view of the polymer structure and protein size featured in our study, this enhancement of protein-resistance should stem from surface phase segregation and the molecular size scale pattern of the incompatible functionalities. The hydrophobic FMA units irregularly distribute in the macromolecule chain of the copolymers, forming a molecular-scale pattern with two different groups alternately arranged. When proteins approach the polymer surface, the hydrophilic domain in the protein will be incompatible with the binding to the hydrophobic part of the polymer and vice versa. In our experiment, BSA and HFg are used as the protein models. BSA is soft and globular with the dimensions of 4 nm × 4 nm × 14 nm,[79] the initial areas for end-on and side-on adsorption would be 56 and 16 $nm^2$, respectively. While fibrinogen is a large and rod-shaped protein with the dimensions of 5 nm × 5 nm × 47 nm,[79] resulting in the side-on and end-on adsorption areas of 235 and 25 $nm^2$, respectively. Maybe that is the reason why surface with similar compositional heterogeneities exhibit different protein adsorption behavior.

Hobara observed that the protein (cytochrome c) preferentially adsorbed on the nanometer-scale hydrophobic 3-mercaptopropionic acid (MPA) domains of the phase-separated mixed SAMs of MPA and 1-hexadecanethiol on flat Au surface.[80] The metal nanoparticles coated with the mixed SAMs, where the size of the ordered phase-separated domains is 5 Å, are extremely effectively in avoiding nonspecific protein adsorption.[81] Muller investigated protein adsorption behaviors on the surfaces containing hyperbranched fluoropolymers (HBFPs) cross-linked with PEG. It was found that surface chemical composition and phase segregation obviously affect the adsorption of human fibrinogen on these surfaces. As the content of PEG increased, the size of the phase-segregated domains of fluorinated moieties became small, fouling by HFg decreased. The antifouling performance of parent HBFPs on the surface was inferior to these amphiphilic surfaces.[82] In our experiment, as expected, BSA adsorption on the amphiphilic surfaces is closely related with that on such molecular-scale pattern and phase segregation. Similarly, although HFg adsorbed on the F3 surface is not the lowest as well as BSA, its adsorption behavior is still affected by the heterogeneous molecular-scale pattern and phase-segregation, which can be seen from Figure 9. These results provide further evidence for our speculation that the molecular-scale heterogeneity and microphase segregation are essential conditions for the antifouling performance detected with the fluorinated amphiphilic copolymers.

Proteins take conformational variation upon adsorbing to a surface.[83,84] The conformation variations are often regarded as the spreading or relaxation of protein, where protein/solid surface contact area varies with surface properties.[85] Figure 9 shows the BSA and HFg adsorption on different fluorinated amphiphilic surface. BSA is a globular protein whose conformation may only be distorted on the interaction with the surfaces.[86] Image A1, B1, C1, D1, E1, and F1 show BSA adsorption on F1, F2, F3, F4, F5, and F6 surfaces. There can be seen that it is hardly for BSA to adsorb on F3 surface, while F1 and F5 surface exhibit a small quantity of adsorbed protein. These results are consistent with XPS measurement. Since the size of BSA is near the scale with the interval sizes of alternating microphase segregation domains of hydrophilic and fluorinated moieties on F3 surface (as shown in Figure 5 image C), it makes us sure that the molecular scale pattern of the surface derived from phase segregation is very important for protein adsorption resistance.

HFg is a rod-shaped protein and has a symmetrical dimeric structure with two sets of three intertwined polypeptide chains, which is easily adsorbed on the hydrophobic surface and takes a flat-topped conformation (the long axis parallel to the surface, a side-on adsorption area of 235 $nm^2$).[79,85] When the surfaces interacted with HFg, low fluorinated moieties content surface displays a better property for protein resistance. According to Figure 5B, HFg could only vertically adsorb (the long axis being vertical to the surface) on surface hydrophobic domains as the

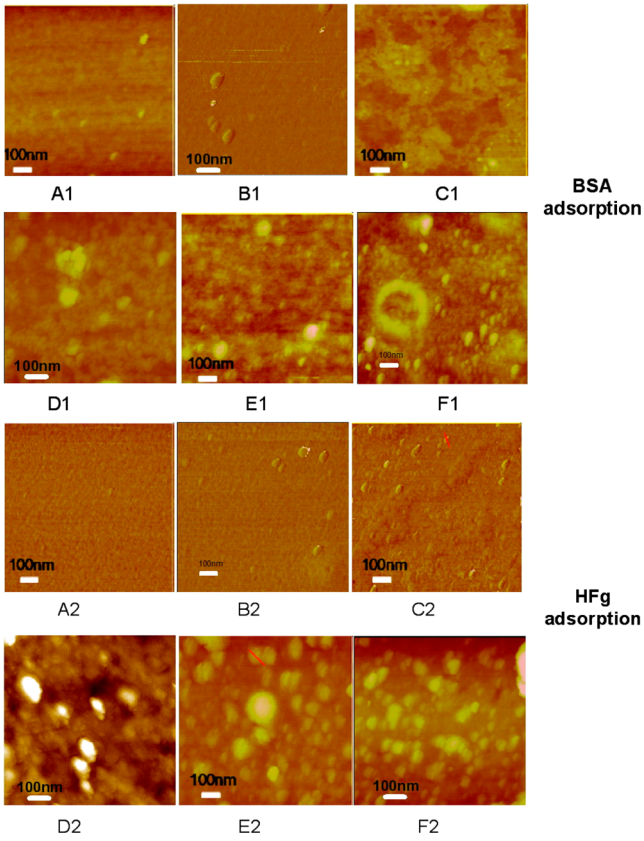


**Figure 9.** AFM tapping height images of F1(A), F2(B), F3(C), F4(D), F5(E), and F6(F) film surfaces after protein adsorption, using BSA(1) and HFg(2) as the proteins model. The areas displayed are 1 $\mu$m × 1 $\mu$m.

size of the hard fluorinated domains is about 5 nm × 5 nm. However, it needs a high energy and strong protein−protein interaction to maintain such a conformation. Hence, it is very hard for HFg to take a flat-topped conformation on this hydrophobic domains, resulting in a very low amount of adsorbed protein. Figure S4 (Supporting Information) shows the morphology of HFg adsorbed on F3 and F5 surfaces. HFg can easily adsorb on the hydrophobic surfaces, when the fluorinated content increase on the surfaces. Therefore the amount of absorbed HFg increases with the enlargement of the fluorinated domains, as seen in Figure 9 image A2 to F2 intuitively.

When the hard hydrophobic region is similar to the size of the HFg molecule, protein can take a flat-topped conformation, as shown on the F3 surface. With the increase of the fluorinated component and the enlargement of hydrophobic region, protein rearrangement further occurs for the enhancement of the surface concentration of protein and protein−protein interaction. These conformation changes also could be found from the AFM images (in Supporting Information Figure S4). Such a rearrangement could be driven by the increase of the hydrophobic interaction of HFgs as their long axes become aligned parallel to each other.[86] Perry interpreted that adsorbed HFgs can reorient and move their long axis perpendicular to the surface due to the increase of hydrophobic interaction between adsorbed proteins.[86] In addition, it should be noted that F1 or F3 exhibit more excellent protein-resistant performance than the PHEMA homopolymer.

According to above results, it is clearly demonstrated that both the surface composition of hydrophilic and fluorinated functionalities and protein molecular-scale heterogeneous pattern on support surface are the crucial factors for antifouling materials. In addition, we further investigated the resistance of bacterial adhesion on these fluorinated amphiphilic copolymers surfaces. The efficiency of the fluorinated amphiphilic surfaces in decreasing bacterial adhesion can be observed from the SEM images in Figure S5 (Supporting Information). Figure S5 shows that all these copolymer surfaces exhibited excellent antifouling ability for *Escherichia coli* (*E. coli*) adhesion. The future work would focus on testing the effectiveness of these amphiphilic copolymer films in more realistic situations, i.e proteins in complex biological fluids or under marine conditions, and we will report such results in our future publication. These results suggest that fluorinated amphiphilic surface with the hydrophilic and the hydrophobic species and heterogeneous patterns on molecular-size scale are related to the understanding and controlling of adsorption of proteins.

## CONCLUSION

Amphiphilic polymers used as antifouling materials have shown to have promising application. Some concepts and opinions are developed to demonstrate the importance of amphiphilic surface structures for preventing biofouling. However, it is still ambiguous to understand the relationship between the antifouing performance and the corresponding surface structure. In this work, a series of noncross-linked amphiphilic copolymers composed of hydrophilic and hydrophobic fluorinated monomers were prepared and then the adsorption behaviors of BSA and HFg on the copolymer surfaces were investigated. All the fluorinated amphiphilic surfaces exhibit excellent protein resistance compared to the hydrophobic PMMA homopolymer. Certain copolymers perform even better than the corresponding hydrophilic PHEMA.

Our results brought about two major conclusions. First, the copolymers whose surface energy lies in the range of the Baier curve present excellent resistance to protein adsorption. Simultaneously, the surface compositional heterogeneities on the molecular size scale with special content of hydrophilic and fluorinated moieties play a significant role in antifouling properties. When the percentage of hydrophilic hydroxyl groups is from 4% to 7% and the percentage of hydrophobic fluorinated moieties is from 4% to 14% on the surface, which is in this two-dimensional region, the copolymers are more unfavorable for protein adsorption than corresponding homopolymers. The second major conclusion is that the protein molecular size scale and the pattern of microphase segregation domains on the support surface strongly affect the adsorption behaviors of proteins. This study has demonstrated the desirable protein-resistant performance of the fluorinated amphiphilic copolymers and provides deeper insight of the effect of amphiphilic surface structures on the protein adsorption behavior.

## ASSOCIATED CONTENT

### Supporting Information

Information concerning the $^1$H NMR spectra of PHEMA-*r*-PFMA and P(HEMA-TMS)-*r*-PFMA, XPS spectra of $N_{1s}$ from PHEMA-*r*-PFMA surfaces after BSA and HFg adsorption, AFM images of HFg adsorbed on sample F3 and F5 surface, and SEM images of *E. coli* adsorbed on fluorinated amphiphilic

copolymers surfaces and other substrates. This material is available free of charge via the Internet at http://pubs.acs.org

## AUTHOR INFORMATION

### Corresponding Author

*E-mail: nhuag@163.com, ypmail2008@sohu.com. Tel.: +86-571-8684-3691.

### Notes

The authors declare no competing financial interest.

## ACKNOWLEDGMENTS

The work was funded by the National Natural Science Foundation of China (NSFC, Nos. 51003097, 51173169, and 50803059). X.L. is grateful for the support from Qianjiang Talents Project of Department of Science and Technology in Zhejiang Province (Grant No. 2011R10025), the Scientific Research Foundation for the Returned Overseas Chinese Scholars, State Education Ministry, and the Zhejiang Province Human Resources and Social Security Bureau.

## REFERENCES

(1) Rabe, M.; Verdes, D.; Seeger, S. *Adv. Colloid Interface Sci.* **2011**, *162*, 87−106.
(2) Huchnall, A.; Rangarajan, S.; Chikoti, A. *Adv. Mater.* **2009**, *21*, 2441−2446.
(3) Page, K.; Wilson, M.; Parkin, I. P. *J. Mater. Chem.* **2009**, *19*, 3819−3831.
(4) Lynch, A. S.; Robertson, G. T. *Ann. Rev. Med.* **2008**, *59*, 415−428.
(5) Hall-Stoodley, L.; Gosterton, J. W.; Stoodley, P. *Nat. Rev. Microbiol.* **2004**, *2*, 95−108.
(6) Bhatt, S.; Pulpytel, J.; Ceccone, G.; Lisboa, P.; Rossi, F.; Kumar, V.; Arefi-Khonari, F. *Langmuir* **2011**, *27*, 14570−14580.
(7) Rana, D.; Marsuura, T. *Chem. Rev.* **2010**, *110*, 2448−2471.
(8) Guo, W. J.; Tang, X. D.; Xu, J.; Wang, X.; Chen, Y.; Yu, F.; Pei, M. S. *J. Polym. Sci., Part A: Polym. Chem.* **2011**, *49*, 1528−1534.
(9) Zolulalian, V.; Zürcher, S.; Tosatti, S.; Textor, M.; Monge, S.; Robin, J−J. *Langmuir* **2010**, *26*, 74−82.
(10) Chang, Y.; Chu, W−L.; Chen, W. Y.; Zheng, J.; Liu, L.; Ruaan, R. C.; Higuchi, A. *J. Biomed. Mater. Res., Part A* **2010**, *93A*, 400−408.
(11) Zhao, C.; Li, L. Y.; Wang, Q. M.; Yu, Q. M.; Zheng, J. *Langmuir* **2011**, *27*, 4906−4913.
(12) Zhang, Z.; Chao, T.; Chen, S. F. *Langmuir* **2006**, *22*, 10072−10077.
(13) Zhang, Z.; Chen, S. F.; Jiang, S. Y. *Biomacromolecules* **2006**, *7*, 3311−3315.
(14) Zhao, C.; Zheng, J. *Biomacromolecules* **2011**, *12*, 4071−4079.
(15) Yarbrough, J. C.; Rolland, J. P.; DeSimone, J. M.; Callow, M. E.; Finlay, J. A.; Call, J. A. *Macromolecules* **2006**, *39*, 2521−2528.
(16) Hu, Z.; Chen, L.; Betts, D.; Pandya, A.; Hillmyer, M. A.; DeSimone, J. M. *J. Am. Chem. Soc.* **2008**, *130*, 14244−14252.
(17) Misra, A.; Jarrett, W. L.; Urban, M. W. *Macromolecules* **2009**, *42*, 7299−7308.
(18) Gao, J.; H, Y. Y.; Ni, H. G.; Wang, L.; Yang, Y. H.; Wang, X. P. *J. Colloid Interface Sci.* **2013**, *393*, 361−368.
(19) Kanno, M.; Kawakami, H.; Nagaoka, S.; Kubota, S. *J. Biomed. Mater. Res.* **2002**, *60*, 53−60.
(20) Kawakami, H.; Kanno, M.; Nagaoka, S.; Kubota, S. *J. Biomed. Mater. Res.* **2003**, *67A*, 1393−1400.
(21) Finlay, J. A.; Krishman, S.; Callow, M. E.; Callow, J. A.; Dong, R.; Asgill, N.; Wong, K.; Kramer, E. J.; Ober, C. K. *Langmuir* **2008**, *24*, 503−510.
(22) Martinelli, E.; Agostini, S.; Galli, G.; Chiellini, E.; Glisenti, A.; Pettitt, M. E.; Callow, M. E.; Callow, J. A.; Graf, K.; Bartels, F. W. *Langmuir* **2008**, *24*, 13138−13147.
(23) Kumar, V.; Pulpytel, J.; Rauscher, H.; Mannelli, I.; Rossi, F.; Arefi-Khonsari, F. *Plasma Proc. Polym* **2010**, *7*, 926−938.
(24) Gudipati, C. S.; F., J. A.; Callow, J. A.; Callow, M. E.; Wooley, K. L. *Langmuir* **2005**, *21*, 3044−3053.
(25) Cho, Y. J; Sundaram, H. S.; Weinman, C. J.; Paik, M. Y.; Dimitriou, M. D.; Finlay, J. A.; Callow, M. E.; Callow, J. A.; Kramer, E. J.; Ober, C. K. *Macromolecules* **2011**, *44*, 4783−4792.
(26) Krishnan, S.; Ayothi, R.; Hexemer, A.; Finlay, J. A.; Sohn, K. E.; Perry, R.; Ober, C. K.; Kramer, E. J.; Callow, M. E.; Callow, J. A.; Fischer, D. A. *Langmuir* **2006**, *22*, 5075−5086.
(27) Krishnan, S.; Wang, N.; Ober, C. K.; Finlay, J. A.; Callow, M. E.; Callow, J. A.; Hexemer, A.; Sohn, K. E.; Kramer, E. J.; Fischer, D. A. *Biomacromolecues* **2006**, *7*, 1449−1462.
(28) Feng, S. J.; Wang, Q.; Gao, Y.; Huang, Y. G.; Qing, F. L. *J. Appl. Polym. Sci.* **2009**, *114*, 2071−2078.
(29) Joshi, R. G.; Goel, A.; Mannari, V. M.; Finlay, J. A.; Callow, M. E.; Callow, J. A. *J. Appl. Polym. Sci.* **2009**, *114*, 3693−3703.
(30) Banerjee, I.; Pangule, R. C.; Kane, R. S. *Adv. Mater.* **2011**, *23*, 690−718.
(31) Martinelli, E.; Menghetti, S.; Galli, G.; Glisenti, A.; Krishnan, S.; Paik, M. Y.; Ober, C. K.; Smilgies, D.-M.; Fischer, D. A. *J. Polym. Sci., Part A: Polym. Chem.* **2009**, *47*, 267−284.
(32) Weinman, C. J.; Gunari, N.; Krishnan, S.; Dong, R.; Paik, M. Y.; Sohn, K. E.; Walker, G. C.; Kramer, E. J.; Fischer, D. A.; Ober, C. K. *Soft Matter.* **2010**, *6*, 3237−3243.
(33) Park, D.; Finlay, J. A.; Ward, R. J.; Weinman, C. J.; Krishnan, S.; Paik, M.; Sohn, K. E.; Callow, M. E.; Callow, J. A.; Handlin, D. L.; Willis, C. L.; Fischer, D. A.; Angert, E. R.; Kramer, E. J.; Ober, C. K. *ACS Appl. Mater. Interfaces* **2010**, *2*, 703−711.
(34) Park, D.; Weinman, C. J.; Finlay, J. A.; Fletcher, B. R.; Paik, M. Y.; Sundaram, H. S.; Dimitriou, M. D.; Sohn, K. E.; Callow, M. E.; Callow, J. A.; Handlin, D. L.; Willis, C. L.; Fischer, D. A.; Kramer, E. J.; Ober, C. K. *Langmuir* **2010**, *26*, 9772−9781.
(35) Krishnan, S.; Ward, R. J.; Hexemer, A.; Sohn, K. E.; Lee, K. L.; Angert, E. R.; Fischer, D. A.; Kramer, E. J.; Ober, C. K. *Langmuir* **2006**, *22*, 11255−11266.
(36) Ma, J.; Bartels, J. W.; Li, Z.; Zhang, K.; Cheng, C.; Wooley, K. L. *Aust. J. Chem.* **2010**, *63*, 1159−1163.
(37) Dimitriou, M. D.; Zhou, Z.; Yoo, H.-S.; Killops, K. L.; Finlay, John. A.; Cone, G.; Sundaram, H. S.; Lynd, N. A.; Barteau, K. P.; Campos, L. M.; Fischer, D. A.; Callow, M. E.; Callow, J. A.; Ober, C. K.; Hawker, C. J.; Kramer, E. J. *Langmuir* **2011**, *27*, 13762−13772.
(38) Wang, Y. P.; Finlay, J. A.; Desimone, J. M. *Langmuir* **2011**, *27*, 10365−10369.
(39) Baxamusa, S. H.; Gleason, K. K. *Adv. Funct. Mater.* **2009**, *19*, 3489−3496.
(40) Gorbet, M. B.; Seften, M .V. *Biomaterials* **2004**, *25*, 5681−5703.
(41) Chen, Y.; Thayumanavan, S. *Langmuir* **2009**, *25*, 13795−13799.
(42) Lazzari, M.; Aglietto, M.; Castelvetro, V.; Chiantore, O. *Chem. Mater.* **2001**, *13*, 2843−2849.
(43) Sugihara, S.; Kanaoka, S.; Aoshima, S. *Macromolecules* **2004**, *37*, 1711−1719.
(44) Kyeremateng, S. O.; Amado, E.; Kressler, J. *Eur. Polym. J.* **2007**, *43*, 3380−3391.
(45) Grignard, B.; Jerome, C.; Calberg, C.; Detrembleur, C.; Jerome, R. *J. Polym. Sci., Part A: Polym. Chem.* **2007**, *45*, 1499−1506.
(46) Churchley, D. P.; Barbu, E.; Ewen, R. J.; Shen, Z.; Kim, Y.; McHugh, M. A.; Zhang, Z. Y.; Nevell, T. G.; Rees, G. D.; Tsibouklis, J. *J. Biomed. Mater. Res., Part A.* **2008**, *84A*, 994−1005.
(47) Betts, D.; Johnson, T.; LeRoux, D.; DeSimone, J. M. *ACS Symp. Ser.* **1998**, *685*, 418.
(48) Oral, A.; Shahwan, T.; Güler, C. *J. Mater. Res.* **2008**, *23*, 3316−3322.
(49) Beers, K. L.; Boo, S.; Gaynor, S. G.; Matyjaszewski, K. *Macromolecules* **1999**, *32*, 5772−5776.
(50) Li, Z.; Day, M.; Ding, J.; Faid, K. *Macromolecules* **2005**, *38*, 2620−2625.
(51) López, G. P.; Ratner, B. D.; Rapoza, R. J.; Horbett, A. T. *Macromolecules* **1993**, *26*, 3247−3253.
(52) López1, G. P.; Chilkoti1, A.; Briggs, D.; Ratner, B. D. *J. Polym. Sci., Part A: Polym. Chem.* **1992**, *30*, 2427−2441.

(53) Ahmed, T. S.; DeSimone, J. M; Roberts, G. W. *Macromolecules* **2008**, *41*, 3086−3097.
(54) Owens, D. K.; Wendt, R. C. *J. Appl. Polym. Sci.* **1969**, *13*, 1741−1747.
(55) Li, X.; Fang, B.; Lin, S.; Wu, P.; Han, Z. *Acta Polym. Sin.* **2003**, *6*, 910−913.
(56) Gitsov, I.; Frechet, J. M. J. *J. Am. Chem. Soc.* **1996**, *118*, 3785−3786.
(57) Ni, H. G.; Li, X. H.; Hu, Y. Y.; Zuo, B.; Zhao, Z. L.; Yang, J. P.; Yuan, D. X.; Ye, X. Y.; Wang, X. P. *J. Phys. Chem. C* **2012**, *116*, 24151−24160.
(58) Nishino, T.; Urushihara, Y.; Meguro, M.; Nakamae, K. *J. Colloid Interface Sci.* **2004**, *279*, 364−369.
(59) Li, K.; Wu, P. P.; Han, Z. W. *Polymer* **2002**, *43*, 4079−4086.
(60) Ni, H. G.; Wang, X. F.; Zhang, W.; Wang, X. P.; Shen, Z. Q. *Surf. Sci.* **2007**, *601*, 3632−3639.
(61) Zhou, Y. X.; Kasi, R. M. *J. Polym. Sci., Part A: Polym. Chem.* **2008**, *46*, 6801−6809.
(62) Nishino, T.; Urushihara, Y.; Meguro, M.; Nakamae, K. *J. Colloid Interface Sci.* **2005**, *283*, 533−545.
(63) Wu, S. *Polymer Interface and Adhesion*; Marcel Dekker: New York, 1982.
(64) Urushihara, Y.; Nishino, T. *Langmuir* **2005**, *21*, 2614−2618.
(65) Yao, F.; Xu, L. Q.; Fu, G. D.; Lin, B. P. *Macromolecules* **2010**, *43*, 9761−9770.
(66) Ming, W.; Tian, M.; van de Grampel, R. D.; Melis, F.; Jia, X.; Loos, J.; van der Linde, R. *Macromolecules* **2002**, *35*, 6920−6929.
(67) Linemann, R. F.; Malner, T. E.; Brandsch, R.; Bar, G.; Ritter, W.; Mülhaupt, R. *Macromolecules* **1999**, *32*, 1715−1721.
(68) Ward, M. D.; Buttry, D. A. *Science* **1990**, *249*, 1000−1007.
(69) Höök, F.; Kasemo, B.; Nylander, T.; Fant, C.; Sott, K.; Elwing, H. *Anal. Chem.* **2001**, *73*, 5796−5804.
(70) Sigal, G. B.; Mrksich, M.; Whitesides, G. M. *J. Am. Chem. Soc.* **1998**, *120*, 3464−3473.
(71) Green, R. J.; Frazier, R. A.; Shakesheff, K. M.; Davies, M. C.; Roberts, C. J.; Tendler, S. J. B. *Biomaterials* **2000**, *21*, 1823−1835.
(72) Muir, B. W.; Tarasova, A.; Gengenbach, T. R.; Menzies, D. J.; Meagher, L.; Rovere, F.; Fairbrother, A.; McLean, K. M.; Hartley, P. G. *Langmuir* **2008**, *24*, 3828−3835.
(73) Ray, S.; Shard, A. G. *Anal. Chem.* **2011**, *83*, 8659−8666.
(74) Wagner, M. S.; McArthur, S. L.; Shen, M.; Horbett, T. A.; Castner, D. G. *J. Biomater. Sci., Polym. Ed.* **2002**, *13*, 407−423.
(75) Baier, R. E. *Biomater., Med. DeVices, Artif. Organs* **1984−85**, *12*, 133−159.
(76) Schrader, M. E. *J. Colloid Interface Sci.* **1982**, *88*, 296−297.
(77) Dexter, S. C. *J. Colloid Interface Sci.* **1979**, *70*, 346−354.
(78) Coelho, M. A. N.; Vieira, E. P.; Motschmann, H.; Möhwald, H.; Thünemann, A. F. *Langmuir* **2003**, *19*, 7544−7550.
(79) Wertz, C. F.; Santore, M. M. *Langmuir* **2001**, *17*, 3006−3016.
(80) Hobara, D.; Imabayashi, S. −I.; Kakiuchi, T. *Nano Lett.* **2002**, *2*, 1021−1025.
(81) Jackson, A. M.; Myerson, J. W.; Stellacci, F. *Nat. Mater.* **2004**, *3*, 330−336.
(82) Gan, D. J.; Mueller, A.; Wooley, K .L. *J. Polym. Sci., Part A: Polym. Chem.* **2003**, *41*, 3531−3540.
(83) Horbett, T. A. *Cardiovasc. Pathol.* **1993**, *2*, S137−S148.
(84) Tanaka, M.; Motomura, T.; Kawada, M.; Anzai, T.; Kasori, Y.; Shiroya, T.; Shimura, K.; Onishi, M.; Mochizuki, A. *Biomaterials* **2000**, *21*, 1471−1481.
(85) Agnihotri, A.; Siedlecki, C. A. *Langmuir* **2004**, *20*, 8846−8852.
(86) Roach, P.; Farrar, D.; Perry, C. C. *J. Am. Chem. Soc.* **2005**, *127*, 8168−8173.